OBSERVATION OF INJECTION AND PRE-ACCELERATION PROCESSES IN THE SLOW SOLAR WIND

GEORGE GLOECKLER

Dept. of Physics and IPST, University of Maryland, College Park, MD 20742, USA, and Dept. of Atmospheric, Oceanic and Space Sciences, University of Michigan, Ann Arbor, MI 48109, USA.

Abstract. Knowledge of injection and pre-acceleration mechanisms of ions is of fundamental importance for understanding particle acceleration that takes place in various astrophysical settings. The heliosphere offers the best chance to study these poorly understood processes experimentally. We examine ion injection and pre-acceleration using measurements of the bulk and suprathermal solar wind, and pickup ions. Our most puzzling observation is that high-velocity tails, extending to at least 60 keV/e – the upper limit of measurements – , are omnipresent in the slow, in-ecliptic solar wind; these tails exist even in the absence of any shocks. The cause of these tails is unknown. In the disturbed solar wind inside CIRs and downstream of shocks and waves these high-speed tails in the distributions of H^+, He^+ and He^{++} become more pronounced and more complex, but with the shapes of the tails showing the same dependence on ion speed for the different species. Pickup hydrogen and helium are found to be readily injected for subsequent acceleration to MeV energies, and thus are the dominant source of CIR-accelerated energetic ions. Competing sources of MeV ions heavier than He are: (1) heated suprathermal solar wind observed downstream of CIR shocks, (2) interstellar N, O and Ne, and (3) the newly discovered heavy pickup ions from an extended inner source inside 1 AU. Our main conclusion is that mechanisms other than the traditional first-order shock acceleration process produce most of the modestly accelerated ions seen in the slow solar wind.

1. Introduction

Capabilities of modern plasma composition spectrometers have made it feasible for the first time to examine processes and mechanisms responsible for the injection and modest acceleration (pre-acceleration) of ions in turbulent regions of the heliosphere. Knowledge of these processes is fundamental for our understanding of the acceleration of particles that is occurring everywhere in the universe. With Ulysses it has been possible to study these mechanisms both in the high-latitude fast solar wind as well as in the in-ecliptic slow wind. Furthermore, the Ulysses orbit and observations around the minimum of the solar cycle provided ample opportunity to study for the first time in some detail ion injection and pre-acceleration mechanisms associated with shocks and turbulence in Corotating Interaction Regions (CIRs) at heliocentric distances where CIRs and corotating shocks become well established. The Solar Wind Ion Composition Spectrometer (SWICS) on Ulysses measures distribution functions of the solar wind and suprathermal ions in the critical velocity range where the injection takes place and acceleration begins. This has enabled us to address such questions as: what conditions lead to the injecting
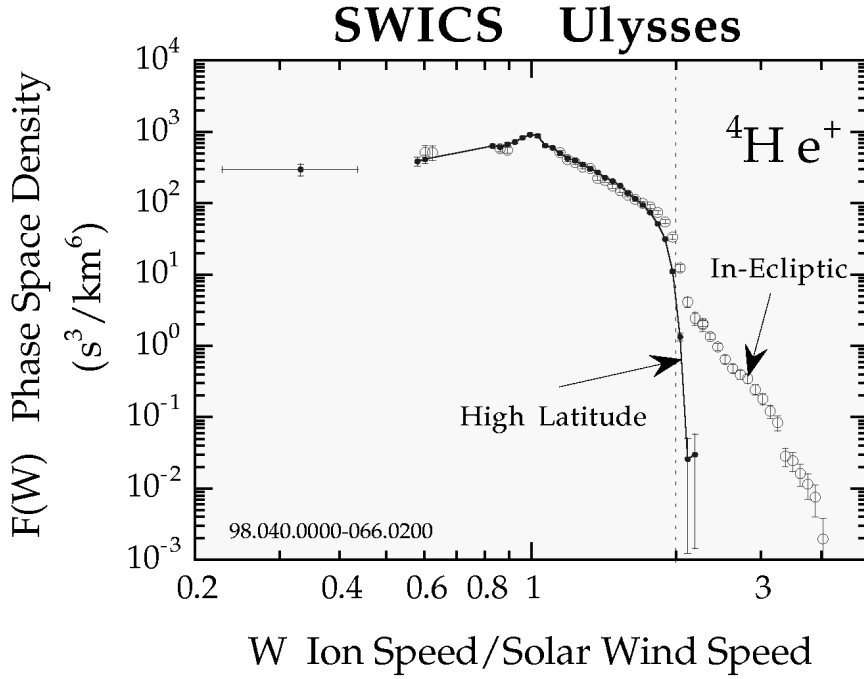
SWICS   Ulysses

Figure 1. Phase space density *vs. W* of interstellar pickup He$^+$ ions in the fast, high-latitude and the slow, in-ecliptic solar wind, respectively. The 100-day averaged high-speed spectrum (April 10 to July 19, 1994) is taken from Gloeckler and Geiss (1998), and shows an abrupt drop in density beyond $W = 2$. The 26-day averaged in-ecliptic distribution, observed in the absence of any shocks and corotating interaction regions (February 9 to March 7, 1998) has a well developed high-speed tail beyond $W = 2$. These distributions were obtained as described by Gloeckler (1996), and the high-speed, high-latitude spectrum was further corrected to remove the $(V_{sw\text{-}hi}/V_{sw\text{-}lo})^4$ dependence of phase space density on solar wind speed (Vasyliunas and Siscoe, 1976) by multiplying the phase space density by 19.

and pre-acceleration of ions (*e.g.* shocks, turbulence or waves), what the basic properties of the injection and pre-acceleration mechanisms are, and what material is accelerated (*e.g.* pickup ions or solar wind). Here we present observations relevant to these questions. In the accompanying paper (Scholer, 1999) the theoretical concepts pertinent to these problems are discussed.

2. Baseline Velocity Distributions of Pickup Ions and the Solar Wind

It is instructive to first establish the characteristic features of baseline velocity distributions (those observed when neither shocks, waves nor CIRs are present) in both the high-speed, high-latitude solar wind and the slow, in-ecliptic wind. The baseline velocity distribution of interstellar pickup He$^+$ observed in the high-speed wind is compared to that in the low-speed wind in Fig. 1. These spectra (phase-
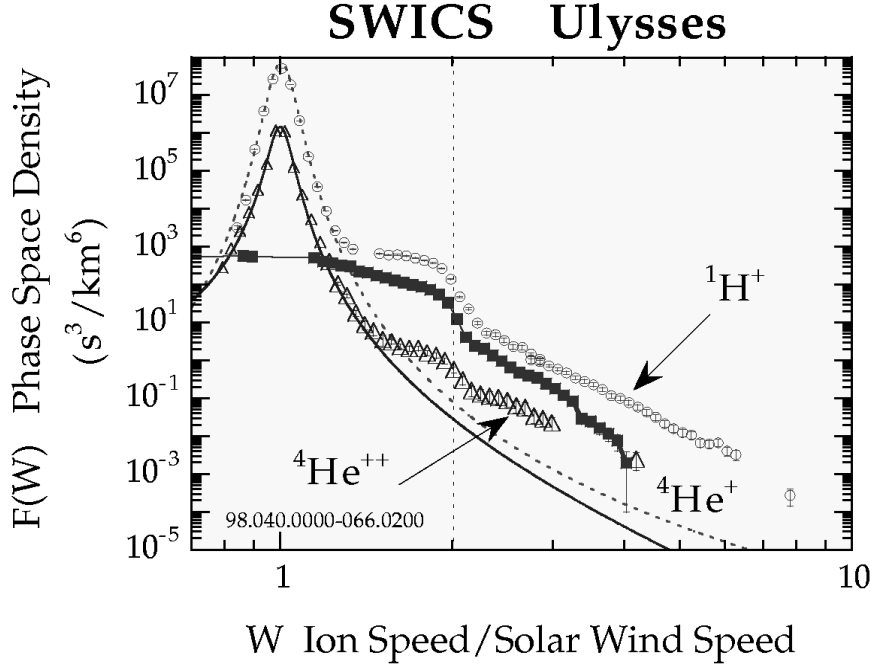
SWICS   Ulysses

Figure 2. Phase space density *vs.* W of H$^+$, He$^+$ and He^{++} ions in the slow (375 km/s), in-ecliptic solar wind (same time period as for Fig. 1). High-velocity tails are clearly visible in all distributions indicating the presence of pre-accelerated ions in the absence of shocks. Suprathermal interstellar pickup H$^+$ and He^{++} rise above the solar wind distributions in the W range between ∼1.5 and 2. For W > 2 ten times more He$^+$ than He^{++} is observed, implying preferential acceleration of the suprathermal pickup ions even in absence of local shocks or waves. Dashed and solid curves are kappa function fits (see *e.g.* Gloeckler and Geiss, 1998, for the definition of the kappa function) to the solar wind H$^+$ ($\kappa = 4.5$) and He^{++} ($\kappa = 3.0$) respectively.

space densities as a function of W, the ion speed divided by the solar wind speed), as well as all data shown here were obtained with the SWICS instrument on Ulysses (Gloeckler *et al.*, 1992). In the absence of acceleration, the pickup ion distributions are expected to have a sharp cut-off at $W = 2$ (*e.g.* Vasyliunas and Siscoe, 1976) as is indeed clearly observed in the high-speed wind (Gloeckler and Geiss, 1998). In contrast to this, the pickup ion distribution in the low-speed, in-ecliptic wind has a well developed high-speed tail above the $W = 2$ cutoff. The density of ions in the tail is of the order of a few percent of the bulk pickup ion distribution.

Strong high-speed tails are also observed in the slow-wind, in-ecliptic baseline velocity distributions of H$^+$ and He^{++} as is illustrated in Fig. 2. The slow-wind He$^+$ spectrum taken from Fig. 1 is shown here for reference. In addition to the bulk solar wind at $W \approx 1$, interstellar pickup H$^+$ and He^{++} are also visible in the W range between ∼1.5 and ∼2. Notice that ten times more He$^+$ than He^{++} is observed for $W > 2$, indicating that pickup ions are preferentially accelerated compared to the bulk solar wind. In the high-latitude fast wind Gloeckler and Geiss
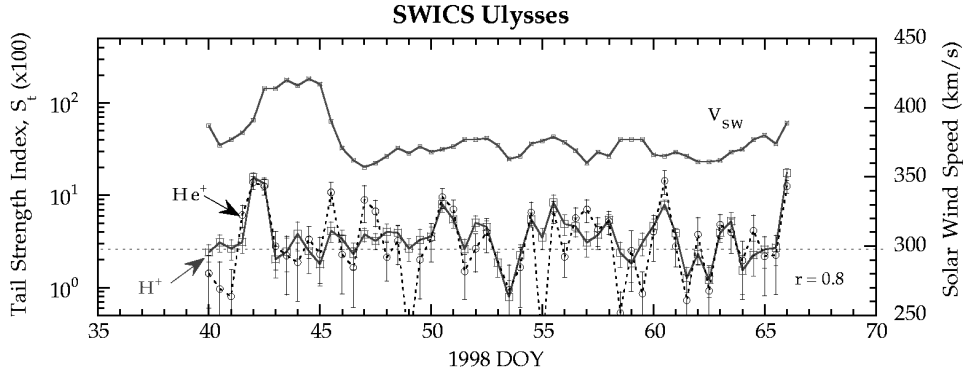
Figure 3. Twelve-hour averages of the tail strength index, S_t (see text), for H^+ and He^+, and solar wind He^{++} speed during a 26-day period when no shocks were observed locally in the in-ecliptic slow solar wind (same time period as for Fig. 1). The two tail strength indices are well correlated and show frequent day-long increases from a baseline value of a few percent.

(1998) found no significant tails in the H^+, He^+ and He^{++} distributions. Thus, the presence of substantial high-velocity tails in the baseline ion velocity distributions in the slow wind is one of many characteristics that distinguishes the low-speed from the high-speed wind.

We investigate next the temporal variability of the strength of suprathermal tails during time periods when no shocks were recorded by Ulysses. The strength of the tail is characterized here by the ratio S_t defined to be the phase space densities of tail ions ($2.0 < W < 3.0$) divided by the phase space density of pickup ions ($1.5 < W < 2.0$). In Fig. 3 twelve-hour averages of the tail strength index, S_t, for both H^+ and He^+, along with the solar wind He^{++} speed are plotted during a baseline time period (February 9 to March 7, 1998). There is a clear correlation (correlation coefficient 0.8) between the S_t of H^+ and He^+ indicating a common cause for the production of ions in the tails (beyond $W = 2$). It is also clear that variations of roughly a factor of five in the S_t of each species are frequently observed. The increases in the density of ions in the tails are not related to local shock acceleration since no shocks waves were recorded at Ulysses during this time period (Balogh and Gosling, personal communication). The possibility that these relatively immobile ions are transported from remote shocks is unlikely, although it cannot be ruled out at present. On the other hand, the tails we observe in the baseline slow solar wind may well be produced by local magnetic field turbulence as reported by Schwadron *et al.* (1996). Future work will investigate possible correlations of S_t with magnetic field direction and turbulence to obtain a better understanding of how suprathermal tails are formed in the absence of shocks and waves in the slow wind.
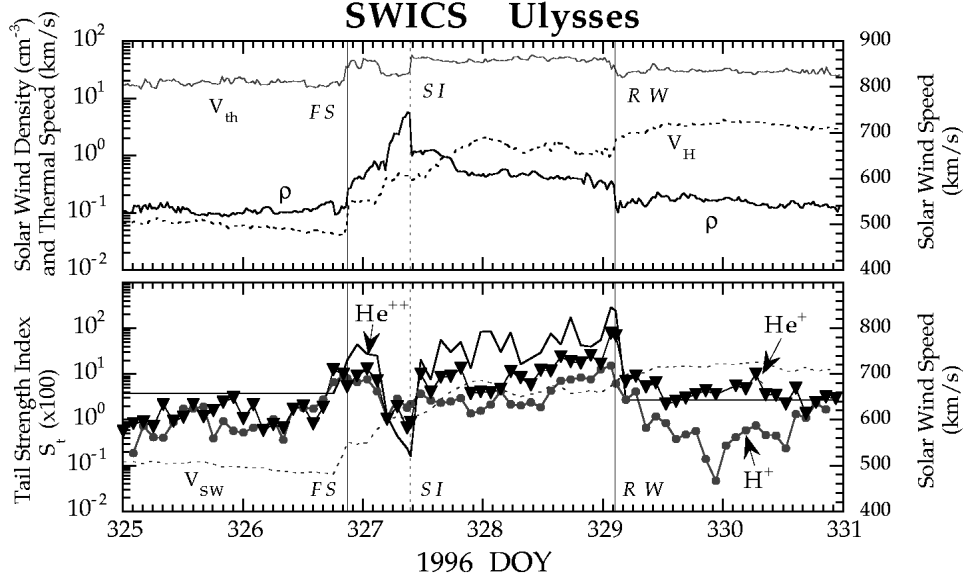
Figure 4. Top panel: 26-minute averages of the solar wind proton density, bulk speed, and thermal speed for a six-day period in December 1996 which includes a forward shock (FS) and reverse wave (RW) of a CIR. The stream interface (SI) is also indicated. *Bottom panel*: Two-hour averaged tail strength indices, S_t, for H^+, He^+ and He^{++}, and solar wind He^{++} speed. The largest increase in all of the S_t (most pronounced tails) is seen around the reverse wave. Baseline values are observed near the stream interface. Horizontal lines indicate upper limits for the He^{++} S_t. The times of the forward shock, reverse wave and stream interface are taken from Wimmer-Schweingruber *et al.* (1999).

3. Acceleration of Suprathermal Ions Near Shocks

It is well established that shocks are able to accelerate particles to very high energies, thus playing a dominant role in producing, for example, cosmic rays. Among the most studied are CIR shocks that cause ions to be accelerated to MeV energies (*e.g.* Keppler, 1998; Maclennan and Lanzerotti, 1998). Ulysses offered the first opportunity to critically examine effects of shocks and waves on various ion species from solar wind energies to several tens of MeV.

Solar wind proton bulk parameters and tail strength indices, S_t, for H^+, He^+ and He^{++} are plotted in Fig. 4 during a six-day time period in late 1996 that contained a CIR. The position of Ulysses at that time was 4.56 AU and 21.4° latitude. The tail strength indices of all species peak around both the forward shock as well as the reverse wave. However, the strongest tails are observed not at the shock but around the reverse wave of the CIR. S_t for He^{++} has its highest value, ~100 times baseline, at the reverse wave. In the upstream regions the tail indices are close to their baseline slow wind values. Downstream they remain high, but dip to their baseline values near the stream interface.

The velocity distribution function for protons for the 40-hour time period downstream of the reverse wave is compared to that upstream of the reverse wave in the
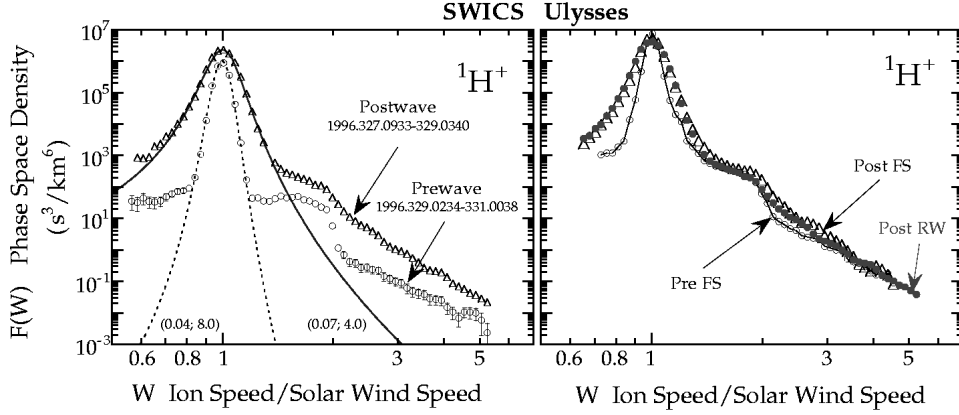
Figure 5. Left panel: Average velocity distributions for H$^+$ upstream (circles) and downstream (triangles) of the reverse wave of the late November 1996 CIR. *Right panel*: Same as the left panel except for the forward shock. The spectrum (corrected for the V_{SW}^4 dependence by multiplying the phase space density by 1.81) downstream of the reverse wave (filled circles) is shown for reference. The two downstream distributions are nearly identical.

left panel of Fig. 5. The upstream distribution looks very much like the baseline slow-wind proton spectrum shown in Fig. 2. The bulk solar wind is mildly non-maxwellian ($\kappa = 8$) and has a low thermal speed ($V_{th}/V_{SW} \approx 0.04$). The interstellar pickup hydrogen distribution with its cut-off at $W = 2$ is well separated from the solar wind distribution and shows little anisotropy due to the nearly perpendicular average magnetic field configuration at these heliocentric distances (Gloeckler *et al.*, 1995). The high-velocity tail above $W = 2$ is also quite evident and extends to the highest speeds measured with SWICS. In contrast to this, the solar wind proton spectrum in the down-stream region (accumulated from the time of observation of the stream interface to that of the reverse wave) has about a factor of two higher thermal speed, and is even more non-maxwellian ($\kappa = 4$). The high-velocity tail is considerably stronger and somewhat steeper than the baseline tail over the entire speed range of SWICS.

In the right panel of Fig. 5 the proton distributions upstream and downstream of the forward shock are compared to the spectrum downstream of the reverse wave. Again the distribution upstream of the forward shock is similar to the baseline distribution, and the tail in the downstream spectrum is both stronger and steeper. The velocity distributions downstream of both the reverse wave and the forward shock are very similar. In comparing the downstream to upstream (baseline) phase space density functions it is apparent that downstream of both the shock and the wave, the density increase in the tail region occurs in the W range between ∼2 and ∼4. Beyond $W \approx 4$ all three spectra appear to be the same.

In our final example we examine injection and pre-acceleration processes associated with a well developed forward and reverse shock pair of a CIR in late December 1992. Ulysses was at 5.08 AU from the Sun at –22.7° latitude. The solar
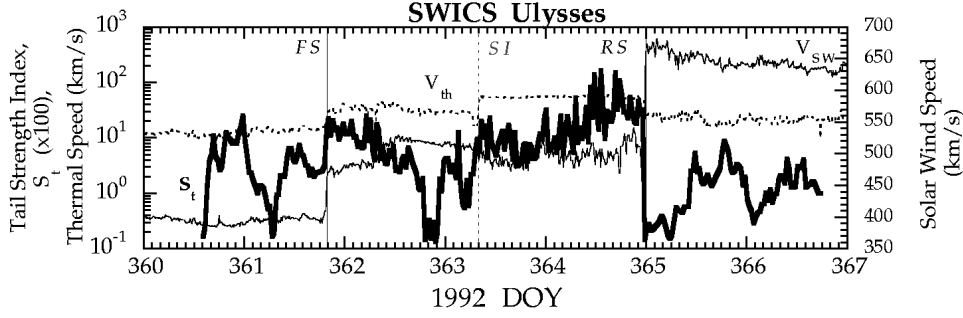
Figure 6. Half-hour averaged ratios of the tail strength index, S_t, (bold solid curve) for He$^+$, and the solar wind He^{++} bulk (light solid curve) and thermal (dotted curve) speeds during a 7-day period that includes the forward and reverse shocks of the late December 1992 CIR. The times for the forward and reverse shocks were taken from Balogh *et al.* (1995). The location of the stream interface was determined by the abrupt decrease of the O^{7+}/O^{6+} ratio measured by SWICS. At both shocks, but especially at the strong reverse shock, S_t increases dramatically and remains high for some period downstream of the shocks. The highest values of S_t are reached six to twelve hours downstream of the reverse shock.

wind bulk and thermal speeds are plotted in Fig. 6 for the seven-day period that includes this 3-day long CIR. At the forward (FS) and reverse (RS) shocks the bulk speed has a sharp jump, and between the shocks the thermal speed (V_{th}) is high attaining its maximum value of close to 60 km/s downstream of the strong, quasi-perpendicular reverse shock ($B_d/B_u = 2.45 \pm 0.27$, $M_S = 2.38$ and $\Theta_{Bn} = 70° \pm 6°$, Balogh *et al.*, 1995). Downstream of the weaker, quasi-parallel forward shock ($B_d/B_u = 1.56 \pm 0.10$, $M_S = 1.55$ and $\Theta_{Bn} = 25° \pm 11°$, Balogh *et al.*, 1995) the solar wind is heated less to an average $V_{th} \approx 30$ km/s.

The tail strength index, S_t, for He$^+$ pickup ions is plotted as the bold solid curve in Fig. 6. Striking features of the curve are the sudden jumps of S_t at the shocks. The jump is especially large (factor of $\sim$100) at the strong reverse shock. However, the highest values of S_t are reached hours downstream of the reverse shock. S_t drops to its baseline lower limit of $\sim 2 \times 10^{-3}$ inside the CIR (1900 to 2200 hours on day 362) between the stream interface and the forward shock. In the upstream regions both the variations and the mean value of S_t are similar to what was found for the baseline slow wind shown in Fig. 3.

In the left panel of Fig. 7 we compare the spectral shapes of H$^+$, He$^+$ and He^{++} measured downstream of the forward shock (FS) with those observed in the downstream region of the reverse shock (RS) in the late December 1992 CIR. The normalization factors applied to the reverse shock data are shown in the figure as fractions in parenthesis. There are several remarkable features apparent from these data. First, we note that more He$^+$ than He^{++} is accelerated even though solar wind alpha particles are at least a factor of 10^3 more abundant than pickup He$^+$. Second, the spectral shapes in the high-speed ($W > 2.4$) tail region behind
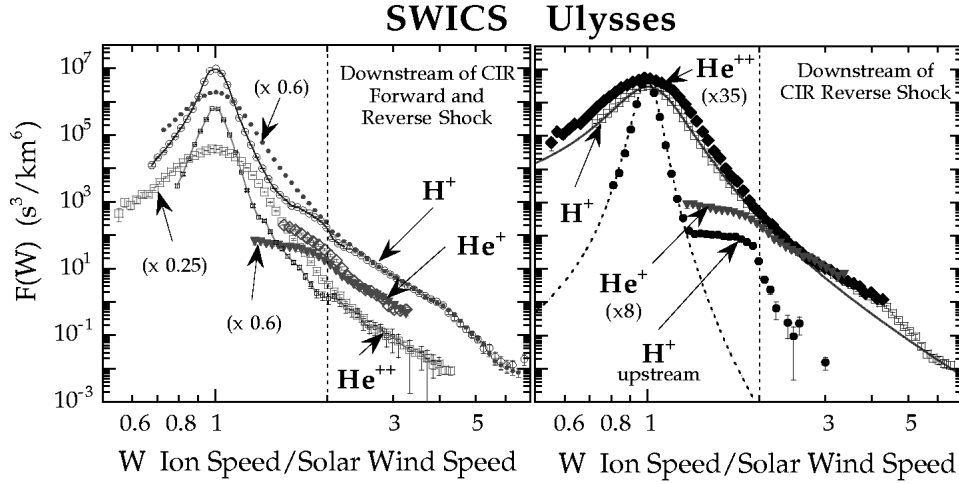
SWICS   Ulysses

Figure 7. Left panel: Distribution functions of H^+, He^+ and He^{++} downstream of the forward shock (open circles, triangles and small squares respectively) and downstream of the reverse shock (filled circles, diamonds and large squares respectively) of the late December 1992 CIR. The time period used for averaging the downstream forward shock spectra was from December 26, 19:41 to December 28, 07:47. For the downstream reverse shock distributions the time interval was December 28, 07:47 to December 29, 23:47. The downstream RS distributions have been multiplied by the fractions shown in parenthesis in order to match the respective spectra in the high-velocity region above $W = 2.4$. Notice the remarkable similarity in the spectral shapes of all three ion species in the high-velocity tail region. *Right panel*: Velocity distributions of H^+ (squares), He^+ (triangles) and He^{++} (filled diamonds) in the region downstream of the reverse shock. The accumulation times were December 28, 07:47 to December 29, 23:47. The He^+ and He^{++} phase-space densities were multiplied by 8 and 35 respectively in order to match the proton spectrum in the high-velocity tail above $W \approx 2.5$. For comparison we also show the proton distribution (filled circles) in the upstream RS region (December 29, 23:47 to January 1, 1993, 00:59). We note that (a) the tails (above $W \approx 2.5$) of all three ion species have the same shape in the downstream region of the shock, and that the shape is not a simple power law as predicted by standard shock acceleration models, (b) the He^+/He^{++} ratio in the tail is ~4.4, and (c) the $H^+/(He^+ + He^{++})$ ratio in the tail is about 6.5.

the reverse shock are identical (within experimental uncertainties) to those behind the forward shock. This is even more remarkable because the two shocks are so different. The forward shock is weaker ($M_S = 1.55$) than the reverse shock ($M_S = 2.38$) and one is quasi-perpendicular while the other quasi-parallel (Balogh *et al.*, 1995). It is evident from the velocity distributions that the solar wind behind the reverse shock is heated more than the wind downstream of the weaker forward shock. In this heated solar wind more suprathermal solar wind ions are available for injection into the acceleration process downstream of the reverse shock than in the region behind the forward shock. The fact that four times more He^{++} and only 1.7 times more H^+ and He^+ is accelerated behind the reverse shock compared to the forward shock implies that downstream of the RS the heated, suprathermal solar wind ions are competitively accelerated along with pickup ions. Behind the forward shock, on the other hand, where the heating is less, fewer suprathermal

solar wind ions are available. Thus, downstream of this relatively weak forward shock the more abundant pickup ions are the principal components available for injection and pre-acceleration.

In the right panel of Fig. 7 we contrast the phase space distribution of protons (open squares) in the downstream region of the CIR reverse shock with that of He^+ (triangles), multiplied by a factor of 8, and He^{++}, multiplied by 35. These normalization factors were chosen so that all three velocity distributions overlapped in the tail region above $W \sim 2.4$. For reference we also show the distribution function of protons (filled circles) measured in the upstream region during the same time period as was used in the left panel. In comparing the upstream to the downstream H^+ distribution we note that the solar wind proton distribution in the downstream region behind the reverse shock is very broad and non-maxwellian. The solid curve is a kappa function fit to protons with $V_{th} = 67.2$ km/s and an extremely low value of $\kappa = 3.1$. This is to be contrasted with the upstream solar wind proton distribution (dotted curve) which is much colder ($V_{th} = 29$ km/s) and has a weaker tail ($\kappa = 4.9$). In the downstream region the pickup hydrogen, quite obvious in the upstream spectrum is completely obscured by the over ten times more abundant heated solar wind protons above $W \sim 1.5$. We therefore conclude that in the case of strong heating illustrated here, mostly suprathermal solar wind protons are injected for further acceleration to higher energies. On the other hand, in instances where less heating occurs (as was shown to be the case downstream of the FS in this CIR and as is often the case behind forward shocks of CIRs in general) the protons in the high-velocity tail will be a mixture of suprathermal solar wind and pickup protons (Gloeckler *et al.*, 1994).

The speed distributions of all three species in the tail region have identical shapes (within experimental uncertainties) above $W \sim 2.4$. This, combined with the fact that the FS and RS spectra also have the same shapes (see left panel of Fig. 7), implies that the acceleration mechanism depends primarily on the ion speed. In addition, the spectral shapes are not simple power laws, as would be predicted by standard shock acceleration models, providing further evidence that the high-velocity tail distributions we observe are not produced by a simple shock acceleration mechanism.

4. Summary and Conclusions

In Table I we summarize our observations of ion injection and pre-acceleration and list the implications that we draw from these measurements. One of our most important findings is that the velocity distributions of H^+, He^+ and He^{++} in the slow, in-ecliptic solar wind free of shocks or waves show well developed high-speed tails indicating the presence of a baseline population of energized ions at all times. In contrast to this, distributions in the quiet high-speed, high-latitude solar wind show little evidence of suprathermal tails (Gloeckler and Geiss, 1998).

TABLE I

Summary of observations of ion injection and pre-acceleration and implications.

Observations	Implications
High-speed tails are always observed in the baseline[a] slow solar wind; they extend to the highest observable energy of SWICS (60 keV/e).	1. Non-shock pre-acceleration takes place in the turbulent in-ecliptic solar wind, or 2. Transport over long distances of ions accelerated by remote shocks.
More He^+ than He^{++} is observed in the high-velocity tails of the baseline slow solar wind	Bulk solar wind is at best a minor source of pre-accelerated particles in the tails.
In the baseline slow solar wind: S_t[b] is variable, S_{tH^+} is correlated with S_{tHe^+}.	Velocity dependent pre-acceleration and/or transport mechanisms.
No evidence for high-speed tails in the baseline high-latitude, high-speed solar wind	Less turbulence, or reduced mobility of ions in the fast, high-latitude wind compared to the slow in-ecliptic solar wind.
S_t of H^+, He^+ and He^{++} increases both near waves and shocks.	Shocks are not required to pre-accelerate ions.
More pre-accelerated He^+ than He^{++} is observed downstream of shocks.	Interstellar pickup He^+ is preferentially accelerated compared to the heated solar wind He^{++}.
Tails in the velocity distributions of different species have identical spectral shapes	Pre-acceleration mechanisms are velocity dependent.
Spectral shapes of tails are complicated; not simple power laws.	Pre-acceleration mechanism is not a simple shock acceleration process.
S_t jumps abruptly at shocks but often reaches its highest values downstream of shocks	Pre-acceleration is not associated with local shock passage.
Density increases occur primarily between $\sim 2 < W < \sim 4$.	CIR pre-acceleration is limited to about 10 keV/amu.
Baseline distributions and tails are observed upstream of CIR shocks.	These tails may well be the seed population for particles accelerated by shocks to MeV energies.

[a] Baseline is defined to be time periods when no shocks, CIRs or waves were observed locally.

[b] $S_t = [F(2.0 < W < 3.0)/F(1.5 < W < 2.0)]$ and is a measure of the strength of a tail. $F(W)$ is the phase space density at speed $W =$ ion speed/solar wind speed.

Thus, in the unperturbed high-speed solar wind few ions above twice the solar wind speed exist. One of the open questions then is how these ubiquitous ions, with speeds nearly ten times that of the solar wind, are created in the slow wind (and not the fast wind) at times when there are no shocks or waves observed locally. Because of their slow mobility, it is unlikely that these ions were accelerated by distant shocks and then transported to the shock free regions of the low-latitude heliosphere, although this possibility cannot be excluded.

Downstream of both the wave and shocks, suprathermal tails increase in strength by one to two orders of magnitude. But the turbulence associated with the wave seems to strengthen the tails as much if not more than that associated with the shock. Again, it appears that it is not the shock itself but rather the strong turbulence (that also heats the solar wind) associated with the shock or the wave that is required for the formation of strong tails. Our observation that the acceleration process produces spectra of identical shapes despite the large difference in the shock parameters once more suggests that the acceleration responsible for the formation of tails is not due to the shocks themselves but rather to the turbulence in the downstream regions of the shocks as was also reported by Gloeckler *et al.* (1994), Gloeckler *et al.* (1995) and Schwadron *et al.* (1996).

We now come to the question of what material is injected and thus further accelerated to MeV energies. The fact that more He^+ than He^{++} is observed above $W \approx 2$ both in the baseline slow wind and in the turbulent regions of CIRs excludes the bulk solar wind (around $W \approx 1$) as a significant source of CIR accelerated energetic particles. As shown in Fig. 7, interstellar pickup ions, in particular He^+, are clearly pre-accelerated in CIRs. This then explains the once puzzling observation by Hovestadt *et al.* (1984) of the ubiquitous energetic (0.4-0.6 MeV/amu) He^+ measured during a $\sim$1.5 year period in 1978/79 at 1 AU. It is very likely that the energetic He^+ they detected was interstellar pickup He^+ accelerated in CIRs at $\sim$3 to $\sim$6 AU and then transported back to 1 AU.

We also provided evidence that the heated solar wind has strong suprathermal tails. Just how much of each of these two populations (interstellar pickup ions and suprathermal solar wind tails) is injected for further acceleration will very likely depend on the relative fraction of these populations in the suprathermal range, perhaps around $W \approx 2$. Since the solar wind is generally heated more behind the reverse shock than it is behind the forward shock (Wimmer-Schweingruber *et al.*, 1997) one would expect that ions accelerated at the reverse shock are predominantly solar wind ions (see Fig. 7). On the other hand, when the solar wind speed is high, interstellar pickup ion distributions extend to higher speeds, and at twice the solar wind speed they may again have densities comparable to or higher than those of solar wind ions heated to these higher speeds. It seems to be the case that in CIRs at $\sim$3 – 6 AU, the heated solar wind distributions for H, He and O and the corresponding interstellar pickup ion distributions have roughly comparable densities near $W \sim 2$ and therefore relatively small changes in either the solar wind thermal speed or its bulk speed will affect the proportion of solar wind versus pickup ions accelerated in CIRs. Observations of the larger relative abundance of energetic (MeV) H and He particles in CIRs compared to that in the solar wind (Gloeckler *et al.*, 1979; Scholer *et al.*, 1979; Reames *et al.*, 1991) support our conclusion that pickup ions form a significant part of the seed population of energetic particles accelerated in these turbulent regions.

The inner source pickup ions could also contribute substantially to the energetic particles accelerated in corotating interaction regions (Gloeckler and Geiss, 1998).

The inner source (Geiss *et al.*, 1995; Geiss *et al.*, 1996) has a carbon to oxygen ratio ∼1. Indeed the average C/O ratio of CIR accelerated particles is also ∼1 (Gloeckler *et al.*, 1979; Scholer *et al.*, 1979; Reames *et al.*, 1991; Fränz *et al.*, 1995). The composition of inner source pickup ions also includes elements such as Mg and Si with an abundance roughly comparable to that of the solar wind (Gloeckler *et al.*, 1999). In fact, Gloeckler *et al.* (1999) argue that inner source pickup ions originate from solar wind absorbed by interplanetary dust and eventually released as slow moving (compared to the solar wind) atoms (Gruntman, 1996) and may be preferentially injected and accelerated at CIRs. Again, the composition of MeV particles heavier than oxygen in CIRs resembles that of the inner source pickup ions (which themselves reflect the composition of the solar wind).

At heliocentric distances of ∼2 to ∼5 AU where CIRs are formed in the lower latitude regions of the heliosphere, it appears that all three sources – interstellar pickup ions, solar wind, and inner source pickup ions – inject more or less comparable amounts of material for further acceleration by CIR shocks. Depending on solar wind conditions one of these sources may predominate. However, at larger heliocentric distances ($> ∼10\,\mathrm{AU}$), the contributions from interstellar pickup ions will grow, while those from both the solar wind and the inner source will diminish. This is consistent with the measured composition of the ∼10 to ∼100 MeV Anomalous Cosmic Rays (ACR) which reflects that of interstellar pickup ions. While most of the acceleration to hundreds of MeVs is likely to take place at the heliospheric termination shock, some pre-acceleration of pickup ions inside the heliosphere is required in order to compensate for adiabatic cooling. The same mechanisms that produce the ever present suprathermal tails in the in-ecliptic slow solar wind in the absence of shocks could also pre-accelerate interstellar pickup ions in the in-ecliptic distant heliosphere right up to the termination shock. Another possibility, suggested by Fisk (1996), is acceleration at distances far beyond ∼10 AU at the interface between the low-speed flow in the ecliptic and the high-speed flow from the polar coronal holes at higher latitudes. Presumably, pickup ions in the turbulence associated with this interface would be pre-accelerated as efficiently as in CIRs. In closing, we believe that one of the outstanding theoretical challenges facing us now is to properly explain the existence of the ubiquitous high-velocity tails that are always so clearly present in the slow, in-ecliptic solar wind.

References

Balogh, A., Gonzalez-Esparza, J. A., Forsyth, R. J., Burton, M. E., Goldstein, B. E., Smith, E. J., and Bame, S. J.: 1995, 'Interplanetary Shock Waves: Ulysses Observations In and Out of the Ecliptic Plane', *Space Sci. Rev.* **72**, 171–180.

Fisk, L. A.: 1996, 'Implications of a Weak Termination Shock', *Space Sci. Rev.* **78**, 129–136.

Fränz, M., Keppler, E., Krupp, N., Rouss, M. K., and Blake, J. B.: 1995, 'The Elemental Composition in Energetic Particle Events at High Heliospheric Latitudes', *Space Sci. Rev.* **72**, 339–342.

Geiss, J., Gloeckler, G., Fisk, L. A. and von Steiger, R.: 1995, 'C^+ Pickup Ions in the Heliosphere and Their Origin', *J. Geophys. Res.* **100**, 23,373–23,377.

Geiss, J., Gloeckler, G., and von Steiger, R.: 1996, 'Origin of C^+ Ions in the Heliosphere', *ISSI Workshop, Space Sci. Rev.* **78**, 43–52.

Gloeckler, G., Hovestadt, D., and Fisk, L. A.: 1979, 'Observed Distribution Functions of H, He, C, O, and Fe in Corotating Energetic Particle Streams: Implications for Interplanetary Acceleration and Propagation', *Astrophys. J.* **230**, L191–L195.

Gloeckler, G., Geiss, J., Balsiger, H., Bedini, P., Cain, J. C., Fischer, J., Fisk, L. A., Galvin, A. B., Gliem, F., Hamilton, D. C., Hollweg, J. V., Ipavich, F. M., Joos, R., Livi, S., Lundgren, R., Mall, U., McKenzie, J. F., Ogilvie, K. W., Ottens, F., Rieck, W., Tums, E. O., von Steiger, R., Weiss, W., and Wilken, B.: 1992, 'The Solar Wind Ion Composition Spectrometer', *Astron. Astrophys. Suppl. Ser.* **92**, 267–289.

Gloeckler, G., Geiss, J., Roelof, E. C., Fisk, L. A., Ipavich, F. M., Ogilvie, K. W., Lanzerotti, L. J., von Steiger, R., and Wilken, B.: 1994, 'Acceleration of Interstellar Pickup Ions in the Disturbed Solar Wind Observed on Ulysses', *J. Geophys. Res.* **99**, 17,637–17,643.

Gloeckler, G., Schwadron, N. A., Fisk L. A., and Geiss J.: 1995, 'Weak Pitch Angle Scattering of few MV Rigidity Ions from Measurements of Anisotropies in the Distribution Function of Interstellar Pickup H^+', *Geophys. Res. Lett.* **22**, 2665–2668.

Gloeckler, G.: 1996, 'The Abundance of Atomic ^{1}H, ^{4}He, and ^{3}He in the Local Interstellar Cloud from Pickup Ion Observations with SWICS on Ulysses', *in* R. von Steiger, R. Lallement, and M. A. Lee (eds.), *The Heliosphere in the Local Interstellar Medium*, Proc. of the First ISSI Workshop, *Space Sci. Rev.* **78**, 335–346.

Gloeckler, G., and Geiss, J.: 1998, 'Interstellar and Inner Source Pickup Ions Observed with SWICS on Ulysses', *Space Sci. Rev.* **86**, 127–159.

Gloeckler, G., Fisk, L. A., Geiss, J., Schwadron, N. A., and Zurbuchen, T. H.: 1999, 'The Elemental Composition of the Inner Source Pickup Ions', *J. Geophys. Res.* in press.

Gruntman, M.: 1996, 'H_2^+ Pickup Ions in the Solar Wind: Outgassing of Interplanetary Dust', *J. Geophys. Res.* **101**, 15,555–15,568.

Hovestadt, D., Klecker, B., Gloeckler, G., Ipavich, F. M., and Scholer, M.: 1984, 'Survey of He^+/He^{2+} Abundance Ratios in Energetic Particle Events', *Astrophys. J. Lett.* **282**, L39–L42.

Keppler, E.,: 1998, 'The Acceleration of Charged Particles in Corotating Interaction Regions (CIR) - A Review with Particular Emphasis on the Ulysses Mission', *Surveys in Geophysics* **19**, 211–278.

Maclennan, C. G., and Lanzerotti, L. J.: 1998, 'Low Energy Anomalous Ions at Northern Heliolatitudes', *Geophys. Res. Lett.* **25**, 3473–3476.

Reames, D. V., Richardson, I. G., and Barbier, L. M.: 1991, 'On the Differences in Element Abundances of Energetic Ions from Corotating Events and from Large Solar Events', *Astrophys. J. Lett.* **382**, L43–L46.

Scholer, M., Hovestadt, D., Klecker, B., and Gloeckler, G.: 1979, 'The Composition of Energetic Particles in Corotating Events', *Astrophys. J.* **227**, 323–328.

Scholer, M.: 1999, 'Injection and Acceleration Processes in Corotating Interaction Regions: Theoretical Concepts', *Space Sci. Rev.*, this volume, 105–114.

Schwadron, N. A., Fisk, L. A., and Gloeckler, G.: 1996, 'Statistical Acceleration of Interstellar Pick-up Ions in Corotating Interaction Regions', *Geophys. Res. Lett.* **23**, 2871–2874.

Wimmer-Schweingruber, R. F., von Steiger, R., and Paerli, R.: 1997, 'Solar Wind Stream Interfaces in Corotating Interaction Regions: SWICS/Ulysses Results', *J. Geophys. Res.* **102**, 17,407–17,417.

Wimmer-Schweingruber, R. F., von Steiger, R., and Paerli, R.: 1999, 'Solar Wind Stream Interfaces in Corotating Interaction Regions: New SWICS/Ulysses Results', *J. Geophys. Res.* **104**, 9,933–9,946.

Vasyliunas, V. M., and Siscoe, G. L.: 1976, 'On the Flux and the Energy Spectrum of Interstellar Ions in the Solar System', *J. Geophys. Res.* **81**, 1,247–1,252.

Address for Offprints: George Gloeckler, University of Maryland, College Park, Maryland 20742, USA (gg10@umail.umd.edu)